Convective Adjustment and Thermohaline Excitability

PAOLA CESSI*

Scripps Institution of Oceanography, La Jolla, California

(Manuscript received 5 January 1995, in final form 2 June 1995)

ABSTRACT

Welander's flip–flop model exhibits oscillations when forced by stochastic white noise (with zero mean) even in the region of parameters where the deterministic system has a globally stable fixed point. Perturbations away from the attracting solutions decay exponentially in time, without any oscillation. Thus, the oscillation that appears when the system is stochastically forced is not related to an eigenfrequency of the linearized system.

The characteristics of this noise-induced oscillation are contrasted with those obtained when the damped harmonic oscillator is forced stochastically. In the case of a stochastically forced damped harmonic oscillator the spectral peak coincides with the frequency of the oscillator, and the amplitude of the oscillations is proportional to the strength of the noise. In the stochastically forced flip-flop model the amplitude of the oscillations is independent of the strength of the noise and the spectral peak moves to lower frequencies as the amplitude of the noise is reduced. Moreover, for noise below a critical threshold, no spectral peak is obtained.

The flip–flop model shares four characteristics with the thermohaline oscillations observed in OGCMs:

1) The freshwater flux determines whether the system oscillates or settles into a steady state. The period of the oscillations is very sensitive to the freshwater flux and becomes arbitrarily long near the transition from steady to periodic behavior.

2) The oscillations are of finite amplitude even just past the threshold value of the freshwater flux that separates periodic behavior from a steady equilibrium.

3) One extremum of the oscillation excursion is close to the value of the steady state that exists below the threshold for transition.

4) When the deterministic system reaches a steady state, oscillations can be excited by adding a stochastic component to the freshwater flux. The period of the resulting oscillations decreases with increasing noise amplitude, while the amplitude of the oscillations is insensitive to the amplitude of the noise.

1. Introduction

Recent results of ocean general circulation models (OGCMs) have indicated that the meridional overturning cell responsible for the bulk of the oceanic heat transport exhibits intrinsic time dependence: the strength of the thermohaline circulation can oscillate in time even if the mechanical and thermodynamical forcing prescribed at the surface are steady.

Weaver et al. (1993) have analyzed an idealized "North Atlantic" circulation model forced by surface wind stress, prescribed freshwater flux, and fast relaxation of the surface temperature to an equilibrium profile. The meridional distribution of the forcing profiles is characteristic of the present North Atlantic. They found that small differences in the freshwater flux at high latitudes lead to different long-time behavior of the meridional overturning cell. Specifically, with one meridional distribution of the freshwater flux the circulation settles into a steady equilibrium.

A different meridional distribution of the freshwater flux leads to sustained oscillations with a period of about 800 years. The addition of a stochastic component to the freshwater flux (white noise in time with zero mean) decreases both the average period and amplitude of the oscillation as the noise variance is increased. Each cycle of the oscillation is characterized by a slow phase where convective adjustment is suppressed and the strength of the meridional circulation is weak, followed by a rapid "flush" with activated convective adjustment and strong meridional overturning.

Mikolajewicz and Maier-Reimer (1990), using the Hamburg global OGCM with complex topography and coastline, have found that the circulation settles into a steady state when driven by smooth forcing fields, but develops large oscillations of the Southern Hemisphere meridional overturning cell when stochastic noise is added to the surface freshwater flux (the average period is 300 years). Pierce et al. (1995) have obtained os-

* Additional affiliation: Istituto FISBAT-CNR, Bologna, Italy.

Corresponding author address: Dr. Paola Cessi, Scripps Institution of Oceanography, University of California, San Diego, Mail Code 0230, La Jolla, CA 92093-0230.
E-mail: cessi@dalek.ucsd.edu

cillations of equal amplitude in the same OGCM without the addition of stochastic noise: reducing the magnitude of the smooth freshwater flux field used by Mikolajewicz and Maier-Reimer (1990) by as little as 8% leads to sustained time dependence with a period of 380 years. Each cycle of the oscillations found by both Mikolajewicz and Maier-Reimer (1990) and Pierce et al. (1995) is characterized by a long period where convective adjustment is active around Antarctica and the southern thermohaline transport is large, followed by a brief phase of interrupted convective adjustment in the same area and weak meridional overturning.

The sensitive dependence of the period and amplitude of oscillations on the freshwater flux has been quantified in the study of Huang and Chow (1994) using the Bryan–Cox model forced by saline forcing alone.

In summary, the centennial and millennial oscillations found in coarse-resolution OGCMs are associated with the activation and suppression of convective adjustment and their existence and periods are extremely sensitive to the freshwater flux.

In this work we reexamine Welander's (1982) flip–flop model because it contains the essential ingredients of thermohaline convective adjustment, and this leads to oscillations whose dependence on parameters share several features with those seen in the OGCMs just mentioned. Specifically, the frequency depends very strongly on the freshwater flux while the amplitude is essentially constant. Moreover, the addition of a stochastic component to the forcing excites almost periodic time dependence. This periodic behavior is nonstandard because the associated deterministic system has no intrinsic time dependence and reaches a stable state via the monotonic decay of exponentially damped perturbations, as opposed to the damped oscillations found, for example, in the Welander–Howard–Malkus loop (Welander 1986). To emphasize this point the aforementioned noise-induced oscillation is compared to that obtained when a weakly damped linear oscillator is excited by stochastic driving.

2. Welander's flip–flop model

In this section the Welander (1982) model is briefly discussed to highlight its essential features and to show that its formulation is equivalent to a simple convective adjustment scheme for a pair of stacked layers at a grid point.

With reference to Welander's (1982) original article we consider the dynamics of two vertically stacked boxes (i.e., two layers at a single grid point), whose density is determined by temperature T and salinity S through a linear equation of state

$$\rho/\rho_0 = 1 + \alpha_S(S - S_0) - \alpha_T(T - T_0). \quad (2.1)$$

The subscript 0 denotes the reference state around which the linearization is done, which is taken here to be the value of all the quantities at the bottom level. Moreover, the bottom box is assumed to be much deeper than the top one so its temperature and salinity do not change appreciably during the timescale of evolution for the upper level. The temperature T and salinity S of the upper box change because the top level is in contact with "the atmosphere," which imposes temperature and salinity fluxes, as well as with the lower box with which properties are exchanged diffusively.

Thus, T and S evolve according to

$$\dot{T} = -\gamma(T - T_A) - \kappa(T - T_0)$$

$$\dot{S} = \frac{F}{H} S_0 - \kappa(S - S_0). \quad (2.2)$$

The temperature is forced using a relaxation condition to a prescribed equilibrium value T_A with a time constant γ^{-1}, while the salinity is forced with a prescribed flux, F, that represents imbalances between evaporation and precipitation plus runoff over the grid point. The depth of the upper level is denoted by H.

Interesting dynamics arises because the vertical diffusion time, κ^{-1}, depends on the vertical density gradient, proportional to $\rho - \rho_0$. Specifically Welander assumes that the diffusive timescale is much longer in stably stratified conditions than for gravitationally unstable stratification. The particular choice made here to model "convection" (one of the cases analyzed by Welander) is

$$\kappa = \begin{cases} \kappa_1 & \text{if} \quad \rho - \rho_0 \leq \Delta\rho \\ \kappa_2 & \text{if} \quad \rho - \rho_0 > \Delta\rho. \end{cases} \quad (2.3)$$

The "nonconvective diffusivity," κ_1, is much smaller than the "convective diffusivity," κ_2, and the threshold density difference, $\Delta\rho$, must be negative in order to regularize the discontinuity introduced in (2.3). A smooth choice for κ as a function of the density difference is discussed by Welander (1982), but the discontinuous prescription in (2.3) is actually more representative of the implementation of convective adjustment in OGCMs.

It should be noticed that in Welander's model convective adjustment is triggered by unstable stratification that is salinity driven. In other words, (2.2) models convection of salty warm over fresh cold water. This scenario is thus appropriate for tropical rather than polar convection. Unstable stratification driven by surface cooling and opposed by surface freshening can be obtained in a modification of Welander's model that includes nonlinearities in the equation of state relating temperature and salinity to density (Winton 1993). Indeed, Pierce et al. (1995) have shown that the oscillations found in the Hamburg OGCM disappear if the equation of state is linearized around a mean temperature and salinity.

Since the goal of this work is to illustrate the features of the oscillations produced by convective adjustment

in the simplest possible case, we have not attempted to include several mechanisms that are demonstrably essential in OGCMs and certainly important in oceanic convection. Thus we use the salinity-driven scenario with a linear equation of state. However, all results presented in this work can be generalized to the case of a nonlinear equation of state and thermally driven convection, without altering the main conclusions.

The system (2.3) is best dealt with in nondimensional variables. We use the definitions

$$x \equiv \frac{T - T_0}{T_A - T_0}, \quad y \equiv \frac{\alpha_S(S - S_0)}{\alpha_T(T_A - T_0)}, \quad t' \equiv t\gamma. \quad (2.4)$$

Equations (2.2) then become

$$\dot{x} = 1 - x - \nu x, \quad \dot{y} = \mu - \nu y. \quad (2.5)$$

The parameter

$$\mu \equiv \frac{F\alpha_S S_0}{H\gamma\alpha_T(T_A - T_0)} \quad (2.6)$$

measures the ratio of the surface salinity flux to the surface temperature flux. In these units $\nu \equiv \kappa/\gamma$ is the ratio of the temperature relaxation time to the vertical diffusion time and is a function of the nondimensional density gradient, $y - x$:

$$\nu = \begin{cases} \nu_1 & \text{if} \quad y - x \leqslant \epsilon, \\ \nu_2 & \text{if} \quad y - x > \epsilon. \end{cases} \quad (2.7)$$

Here $\nu_1 \equiv \kappa_1/\gamma$ is assumed to be much smaller than one because the diffusion time in stably stratified conditions, κ_1^{-1}, is much longer than γ^{-1}, which is typically chosen as several days. Here $\nu_2 \equiv \kappa_2/\gamma \gg \nu_1$ is of order one or larger because in unstably stratified conditions, vertical mixing is of order one day (Jones and Marshall 1993). Finally, $\epsilon \equiv \Delta\rho_0/[\alpha_T(T_A - T_0)]$ is a small negative number, representing the threshold vertical density gradient beyond which convection occurs.

The behavior of the system (2.5) is controlled by a single parameter, μ, the nondimensional salinity flux defined in (2.6). For $\mu_2 > \mu > \mu_1$, with

$$\mu_1 \equiv \frac{\nu_1}{1 + \nu_1} + \epsilon\nu_1$$

$$\mu_2 \equiv \frac{\nu_2}{1 + \nu_2} + \epsilon\nu_2, \quad (2.8)$$

the system oscillates periodically. For values of μ outside the range indicated in (2.8) a globally attracting stable fixed point is reached. A more detailed discussion of the stable states is given in the original work by Welander (1982). We now analyze the system when the parameter μ is close to one of the critical values; that is, $\mu = \mu_2 - \nu_2\delta$ and δ is much less than unity. For $\delta < 0$, a fixed point is reached where convection is always active; that is, $\nu = \nu_2$. In this case temperature and salinity are decoupled in (2.5), and because there are only relaxation processes, the fixed point is approached through a direct exponential decay and not with a damped oscillation. If $\delta > 0$, the steady solution disappears (i.e., it no longer exists) and, instead, a thermohaline oscillation is established. This is a global bifurcation because the oscillation immediately has finite amplitude and the steady solution ceases to exist, rather than merely losing stability.

The calculation of the period of oscillation for $\delta > 0$ is rather complicated even when $\delta \ll 1$. In that limit, the oscillation has a fast portion and a slow relaxation part as shown in Fig. 1, and this allows some simplifications. The details of the calculations to obtain the approximate period are given in appendix A. The final result is that the period, τ, is

$$\tau = -(\nu_2)^{-1} \ln(\delta) + (\nu_2)^{-1} \ln(y_{\max} - \mu/\nu_2) + O(\delta^{1/\nu_2}); \quad (2.9)$$

$y_{\max}(\nu_1, \nu_2, \mu, \epsilon)$ indicates the maximum value that the salinity gradient reaches during the oscillation. Numerical values of $y_{\max}$ are given in the appendix. Here we just remark that $y_{\max}$ is approximately independent of δ when $\delta \ll 1$. The minimum value of y is $y_{\min} \approx \mu_2/\nu_2$. Notice the logarithmic dependence of the period, τ, on the distance to the critical value of the controlling parameter, δ. The logarithm is standard for transitions where a fixed point ceases to exist [referred to as "hard" loss of stability by Arnold (1992) and

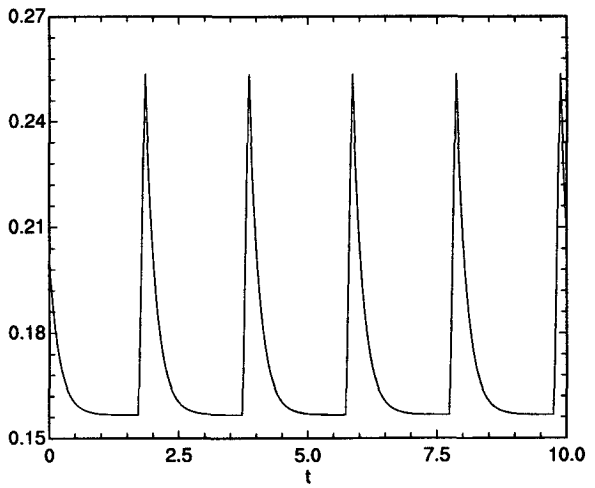

FIG. 1. A typical time series of the salinity gradient, y, solution of Welander's flip–flop model in the oscillating regime. With reference to the nondimensional equations (2.5) and (2.7), the parameters values are $\mu = 0.7833$, $\nu_1 = 0.1$, $\nu_2 = 5.0$, $\epsilon = -0.01$. The critical values for the onset of oscillations, defined in (2.8), are $\mu_1 = 0.089909$ and $\mu_2 = 0.78\overline{3}$. In this case the salinity flux μ is very close to μ_2, the threshold value beyond which the system reaches the "always convecting" fixed point. The salinity gradient, y, slowly relaxes toward the fixed point μ_2/ν_2 until it reaches a low enough value for "convection" to halt. During the brief "nonconvecting" phase, y quickly jumps to the value $y_{\max}$ where convection is reestablished.

Andronov et al. (1966)] and is not an artifact of the discontinuity in (2.7). Thus, even if the period of the oscillation scales with the short convective adjustment time, it can be as long as infinity depending on how small δ is. This is the first point of contact between (2.5) and the general circulation models described in the introduction: the period of the thermohaline oscillations is extremely sensitive to the freshwater forcing and can be made arbitrarily long by operating close to the critical values μ_1 and μ_2.

The amplitude of the oscillation, as quantified by $y_{max} - y_{min}$ with reference to Fig. 1, is given by

$$y_{max} - y_{min} = \begin{cases} \text{const} + O(\delta) & \text{if} \quad \delta \geq 0 \\ 0 & \text{if} \quad \delta < 0. \end{cases} \tag{2.10}$$

This is the second point of contact of the flip–flop model with OGCMs: the amplitude of the oscillations is finite even just past the transition threshold (cf. Huang and Chow 1994 and Pierce et al. 1995).

The results in (2.9) and (2.10) should be contrasted with the analogous expression for a nonlinear system that has a "soft" loss of stability as a control parameter is varied. A generic example is the van der Pol–Duffing oscillator:

$$\ddot{y} + (-\delta + y^2)\dot{y} + \Omega^2 y + y^3 = 0. \tag{2.11}$$

Here the control parameter is δ, the linear damping coefficient. Sustained nonlinear oscillations are obtained for positive δ. Then, for small negative damping, that is, $0 < \delta \ll 1$, the period of the oscillation, again denoted with τ, is

$$\tau = 2\pi/\Omega + O(\delta), \tag{2.12}$$

and the amplitude of the oscillation is

$$y_{max} - y_{min} \sim \sqrt{\delta}. \tag{2.13}$$

To summarize, we have contrasted two types of bifurcation from a steady solution to an oscillation as a control parameter δ is varied. There is the "hard" loss of stability, associated with Andronov's name, and the "soft" loss of stability, associated with Hopf's name. We emphasize that the two bifurcations can be recognized by the quantitative dependence of the period τ on the control parameter δ [cf. (2.9) with (2.12)]. In addition the dependence of the amplitude of the oscillation on δ is qualitatively different in the two cases [cf. (2.10) with (2.13)].

Finally, we remark that in the oscillations stemming from a Hopf bifurcation, y_{max} and y_{min} *straddle* the value of the fixed point that was stable for positive damping. But in the oscillations stemming from a hard loss of stability, one of the extrema, for example y_{min} in Fig. 1, is close to the value of the fixed point that existed for negative criticality δ. Thus in the hard case the oscillations "bounce" on one side of the fixed point as in Fig. 1. This is the third point of contact between the flip–flop model and OGCMs: the relaxation–oscillations typically have one extremum very close to the steady state found below the freshwater flux threshold (cf. Fig. 3c in Huang and Chow 1994).

Another feature of the Welander flip–flop periodic solution when $0 < \delta \ll 1$ is the relaxation–oscillation character of each pulse, that is, a slow relaxation toward an equilibrium and a fast escape away from it (cf. Fig. 1). Once again this is neither an artifact of the discontinuous structure of the diffusivity ν nor of the large difference between the "convective" and "weakly diffusing" mixing timescales. Indeed, in the case shown in Fig. 1, the slow relaxation occurs during the "convective" phase, with a timescale proportional to ν_2^{-1} [cf. Eq. (2.9)]. The fast escape occurs during the "nonconvective" phase (when the mixing is slow and $\nu = \nu_1$), and is nevertheless much shorter than the convective phase (cf. the second and third columns of Table 1).

Near the onset of the limit cycle at the other end of the parameter range defined in (2.8), that is, for μ close to μ_1, the slow relaxation portion of the oscillation is obtained during the nonconvective phase, while the fast jump operates during convection, that is, when the salinity exceeds a maximum value (cf. Fig. 2). For expository reasons, we limit ourselves to the analysis in the case where μ is close to μ_2 defined in (2.8).

The relaxation–oscillation behavior is a generic characteristic of the transition leading to the disappearance of a fixed point (as opposed to becoming unstable), and the emergence of a globally attracting limit cycle of finite amplitude. It suggests a simplified reformulation of Welander's model, appropriate when the criticality δ is small.

3. The "convective adjustment" model

Any reader who has diligently reproduced the algebra in the appendix will appreciate the need for further simplification of the flip–flop model.

We replace the system (2.5) and (2.7) with a single equation for the salinity gradient, y:

TABLE 1. The duration of the short nonconvective phase, t^*, of the long convective phase, τ, and the maximum and minimum salinity gradient, y_{max} and y_{min}, as a function of the salinity flux, μ in the Welander flip–flop. The other parameters are $\nu_1 = 0.1$, $\nu_2 = 5.0$, $\epsilon = -0.01$. The critical values separating stationary from periodic behavior, defined in (2.8), are $\mu_1 = 0.089\overline{09}$ and $\mu_2 = 0.78\overline{3}$.

μ	t^*	τ	y_{max}	y_{min}
0.7833333	0.1253211	∞	0.2522711	0.1566666
0.7641242	0.1728026	0.6322213	0.2867578	0.1585659
0.7449152	0.2212076	0.5380028	0.3202875	0.1608345
0.7257062	0.2713328	0.4935464	0.3530945	0.1632032
0.7064971	0.3234446	0.4666811	0.3852082	0.1656228
0.6872881	0.3777398	0.4482535	0.4166249	0.1680751

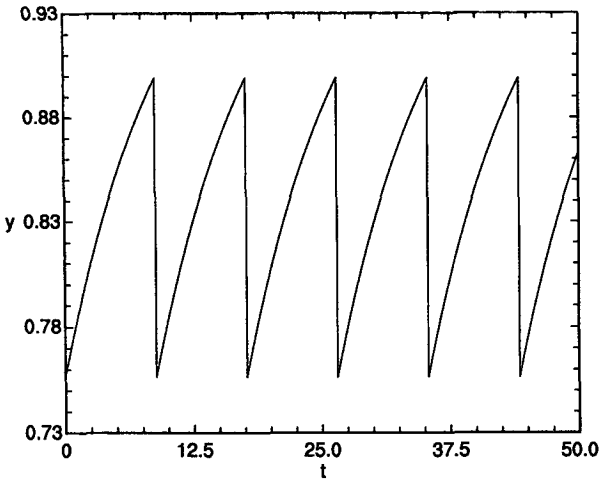

FIG. 2. As in Fig. 1 except that $\mu = 0.1$; that is, the salinity flux μ is close to μ_1, the threshold value beyond which the system reaches the "never convecting" fixed point. The salinity gradient, y, relaxes toward the "never convecting" fixed point, μ_1/ν_1, until it reaches a high enough value for convection to start. During the short "convecting" phase, y quickly falls to a small enough value for convective adjustment to stop. In this case the short phase of the oscillation occurs during convective adjustment, while for the parameters value of Fig. 1, the "nonconvecting" portion is fast.

$$\dot{y} = \begin{cases} \mu - \nu_2 y & \text{if} \quad y \geq \mu_2/\nu_2 \\ y \to y_{\max} & \text{if} \quad y < \mu_2/\nu_2. \end{cases} \tag{3.1}$$

In (3.1) $y_{\max}$ is taken to be a constant, that is, the value $y_{\max}$ at $\delta = 0$ in Table 1, μ and ν_2 are the same parameters used in section 2. The convective adjustment system (3.1) replaces the *short* phase when convection is halted (this occurs when the surface salinity, y, falls below $y_{\min} \approx \mu_2/\nu_2$) with an *instantaneous* adjustment to the maximum value allowed by stable stratification, $y_{\max}$. Counterintuitively, the slow phase of the pulse, when μ is close to μ_2 defined in (2.8), is when convection is occurring and the fast portion is when convection is halted. Because for small δ both $y_{\max}$ and $y_{\min}$ are approximately independent of δ, the system (2.5) and (2.7) can be replaced with a single equation for the salinity gradient, y, (we could have equally used the temperature gradient, x).

The advantage of the "adjustment" model (3.1) is its extreme simplicity. When $\mu > \mu_2$, the solution is

$$y(t) = \frac{\mu}{\nu_2}(1 - e^{-\nu_2 t}) + y(0)e^{-\nu_2 t}; \tag{3.2}$$

that is, the system settles into a steady state where the vertical salinity gradient is small because convection is always operating. Notice that the fixed point is reached through monotonic decay and not via a damped oscillation.

On the other hand, when $\mu < \mu_2$, the fixed point is below the threshold where the density is unstably stratified and convection halts temporarily. The vertical salinity gradient oscillates with period

$$\tau = -(\nu_2)^{-1}[\ln(\delta) - \ln(y_{\max} - \mu/\nu_2)], \tag{3.3}$$

the same value obtained in the two-term approximation (2.9) of Welander's model. The salinity gradient is

$$y(t) = \frac{\mu}{\nu_2}[1 - e^{-\nu_2(t-n\tau)}] + y_{\max}e^{-\nu_2(t-n\tau)} \tag{3.4}$$

with $n\tau \leq t < (n+1)\tau$. Figure 3 shows $y(t)$ in the oscillating regime. The salinity gradient is discontinuous at times $t = n\tau$ because the adjustment model replaces the fast phase of the oscillation with an instantaneous jump up to $y_{\max}$.

The approximation (3.1) of Welander's model, valid in a small but revealing region of the controlling parameter, μ, is a very simple convective adjustment scheme for a single component of the density. When the density gradient falls below a threshold value, appropriate for the halting of convection, it is instantaneously adjusted to a positive value and obeys "convection" dynamics. Incidentally, for the adjustment model (3.1), the period is $\tau \sim \delta^{-1}$ when $\delta \gg 1$. In other words, the *frequency* of the oscillation is proportional to $\mu_2 - \mu$, when $\mu \ll \mu_2$. The frequency, $\omega = 2\pi/\tau$, and the maximum and minimum excursions, $y_{\max}$, and $y_{\min}$, of the oscillation in the adjustment model (3.1) are plotted in Fig. 4 as a function of the nondimensional salinity flux, μ, for a range of values encompassing both large and small criticality δ. Figure 4 is in qualitative agreement, perhaps by coincidence, with the findings of the careful numerical study of Huang and Chou (1994) (cf. Figs. 3a and 3c of Huang and Chou 1994). Finally, Fig. 5 shows schematically the frequency and the minimum and maximum salinity gra-

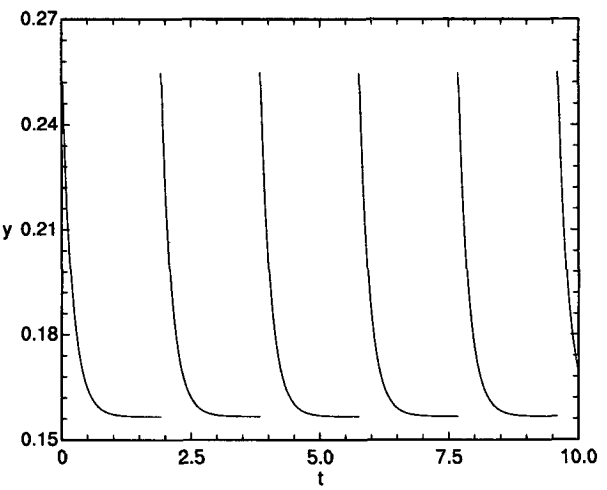

FIG. 3. A typical time series of the salinity gradient, y, solution of the "convective adjustment" model (3.1) in the regime of periodic behavior. The parameter values are $\mu = 0.7833$, $\nu_2 = 5.0$, $y_{\max} = 0.252$, and $\mu_2 = 0.78\overline{3}$. The period and amplitude of oscillations are very close to those obtained with the Welander's model for the same parameters (cf. Fig. 1).

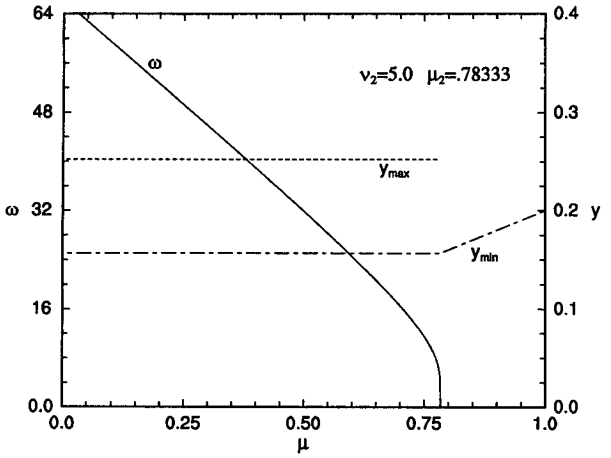

FIG. 4. The frequency ω, (solid line), the maximum salinity gradient y_{max}, (dashed line), and the minimum salinity gradient y_{min} (double-dashed line) of the oscillations in the convective adjustment model (3.1) as a function of the nondimensional salinity flux μ. The left-hand axis refers to the values of ω and the right-hand axis to the values of y_{max} and y_{min}. The parameter values are $\nu_2 = 5.0$, $y_{max} = 0.252$, and $\mu_2 = 0.783$. For $\mu \geq \mu_2$, ω is approximately $-2\pi\nu_2/\ln(\mu_2 - \mu)$. For $\mu \ll \mu_2$, ω is approximately $2\pi(\mu_2 - \mu)(y_{max} - \mu_2/\nu_2)^{-1}$. There are no oscillations for $\mu \geq \mu_2$, and the salinity gradient reaches the fixed point $y = y_{min} = \mu/\nu_2$. The convective adjustment model is a local approximation of the flip–flop model valid for $\mu \approx \mu_2$ (cf. Fig. 5).

dient as a function of the salinity flux in Welander's model (2.5). The dependence is more complicated than in the adjustment model because there are *two* critical values of μ separating periodic from stationary behavior. But again we emphasize that at both these critical values $\omega \to 0$, or the period becomes infinite.

In the following we will restrict our attention to the range where the salinity flux μ is close to μ_2: this is the range of parameters where the adjustment model (3.1) and Welander's model are in quantitative agreement. The adjustment model allows a relatively detailed analysis of the results when the salinity flux μ has a stochastic component.

4. Statistical description of the stochastically forced adjustment model

In this section we consider μ in (3.1) to have a random time-dependent component with zero mean and with simple statistical properties. We thus set

$$\mu = \bar{\mu} + \mu'(t). \tag{4.1}$$

This implies, for the original Welander system (2.2), that the freshwater flux F is time dependent, while the "equilibrium" temperature T_A is fixed to a constant value. In order to approximate $\mu'(t)$ with white noise, Eq. (3.1), repeated here for convenience,

$$\dot{y} = \begin{cases} \bar{\mu} + \mu'(t) - \nu_2 y \\ \qquad \text{if} \quad y \geq \mu_2/\nu_2, \\ y \to y_{max} \\ \qquad \text{if} \quad y < \mu_2/\nu_2, \end{cases} \tag{4.2}$$

is discretized in time with the forward Euler scheme. At each time step $\mu'(t)$ is extracted from a random Gaussian distribution with zero mean and variance

$$\langle \mu'^2 \rangle = \sigma^2/dt. \tag{4.3}$$

The brackets indicate an ensemble average and dt is the size of the time step.

The autocorrelation function

$$\langle \mu'(s)\mu'(s+t) \rangle = \begin{cases} (1 - t/dt)\sigma^2/dt, \\ \qquad \text{if} \quad t \leq dt \\ 0, \qquad \text{if} \quad t > dt \end{cases} \tag{4.4}$$

approximates a delta function when $dt \ll 1$. The stochastic component of the salinity flux induces interesting behavior when $\bar{\mu} = \mu_2 - \delta$, with $|\delta| \ll 1$ and δ *negative*. This is the range of parameter where the associated deterministic system (3.1) reaches a fixed point, $y = \bar{\mu}/\nu_2$, but it is close to the threshold where periodic behavior is found. Figure 6 shows two time series of $y(t)$ obtained integrating (4.2) with (solid line) and without (dashed line) the stochastic compo-

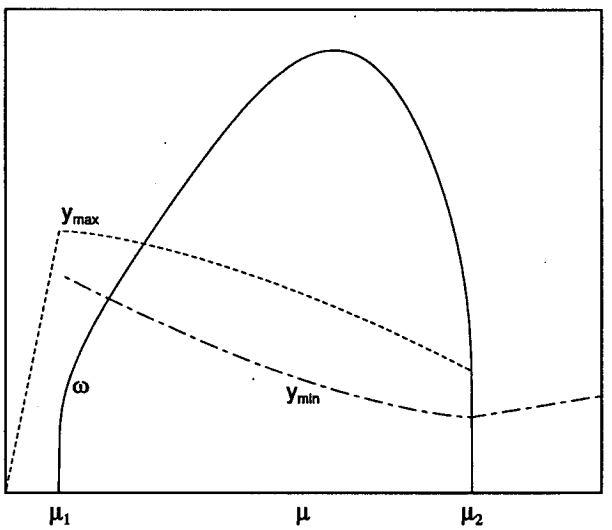

FIG. 5. A qualitative sketch of the frequency ω (solid line), maximum salinity gradient y_{max}, (dashed line), and minimum salinity gradient y_{min} (double-dashed line) of the oscillations in the flip–flop model (2.5) as a function of the nondimensional salinity flux μ. For μ just greater than μ_1 the frequency is approximately $\omega \approx -2\pi\nu_1/\ln(\mu - \mu_1)$, and the amplitude, $y_{max} - y_{min}$, is approximately constant. For μ just smaller than μ_2, $\omega \approx -2\pi\nu_2/\ln(\mu_2 - \mu)$ and $y_{max} - y_{min}$ is approximately constant. There are no oscillations for either $\mu \leq \mu_1$ (the salinity gradient reaches the fixed point $y = y_{max} = \mu/\nu_1$) or $\mu \geq \mu_2$ (the salinity gradient reaches the fixed point $y = y_{min} = \mu/\nu_2$).

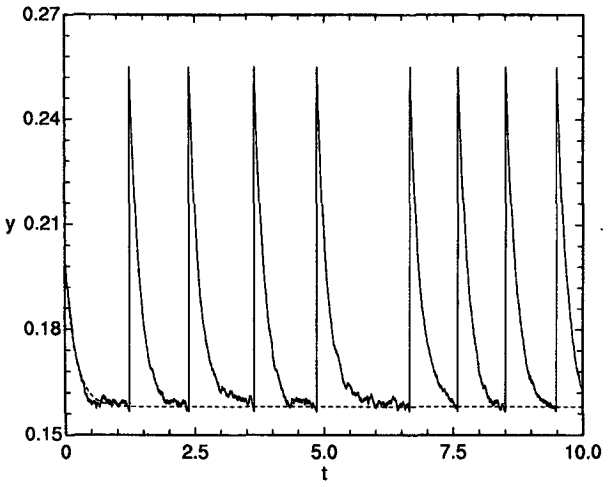

FIG. 6. Two time series of the salinity gradient, y, solution of the convective adjustment model (4.2) with (solid curve) and without (dashed curve) stochastic flucuations of the salinity flux μ. The parameter values are $\bar{\mu} = 0.79$, $\nu_2 = 5.0$, $y_{max} = 0.252$, and $\mu_2 = 0.78\overline{3}$ for both curves. The variance of the stochastic forcing μ', defined in (4.3), is $\sigma = 0.0047434$, the time step is $dt = 1 \times 10^{-3}$. The random forcing excites a quasi-periodic oscillation (solid line), which is absent in the associated deterministic system (dashed line).

nent, μ', of the salinity flux. The random forcing excites a series of pulses, each with a well-defined duration and amplitude, but separated by intervals whose average duration depends on the amplitude of the noise. Specifically, the duration of the intervals between pulses in Fig. 6 is a random variable, but clearly its standard deviation is smaller than the mean. Integration of the Welander model (2.5) and (2.7) for the same parameter values with and without noise shows the same behavior.

The time series plotted with a solid line in Fig. 6 should be contrasted with that obtained by stochastically exciting a damped oscillator, or even a more complex system below the threshold of a Hopf bifurcation, for example, Yang and Neelin (1993). In the latter case the noise-induced oscillations have a well-defined period, independent of the noise, while the *amplitude* is a random variable. In Fig. 6 the amplitude of each pulse is independent of the noise (this is also approximately true when the flip–flop model is used), and the spacing of the pulses is approximately constant in time.

The mechanism through which random fluctuations induce an oscillation in the convective adjustment model is the following. The deterministic system decays exponentially toward the attracting point $y = \bar{\mu}/\nu_2$ and the stochastic forcing produces jiggles around this equilibrium. If one of these fluctuations carries the system to $y = \mu_2/\nu_2$, then a pulse is generated by the convective adjustment. The duration of this pulse is given by the deterministic dynamics: y decays exponentially back toward the attracting point $y = \bar{\mu}/\nu_2$.

This qualitative picture indicates that there are two small parameters:

(i) the distance between the attracting point $y = \bar{\mu}/\nu_2$ and the threshold $y = \mu_2/\nu_2$: $\delta \equiv (\mu_2 - \bar{\mu})/\nu_2$

(ii) the amplitude of the random "rattling" around the attracting point:

$$\Delta \equiv \sigma/\sqrt{\nu_2}. \tag{4.5}$$

In order to produce a roughly evenly spaced sequence of pulses, such as that in Fig. 6, one must have $\Delta \gtrsim \delta$ so that the rattling moves the system to the threshold almost as soon as the deterministic dynamics brings it into the neighborhood of $y = \bar{\mu}/\nu_2$. If $\Delta \ll \delta$, then the rattling is weak and the system waits for a rare, large fluctuation to carry it to the threshold $y = \mu_2/\nu_2$. Thus, in this second case the pulses are separated by long intervals of mere rattling around the equilibrium.

In summary, almost periodic behavior, and thus a spectral peak, is obtained only if $\Delta \gtrsim \delta$: Fig. 7 shows the spectrum of a time series analogous to that of Fig. 6. In the regime $\Delta \ll \delta$ the spectrum exhibits no peak (see Fig. 8), and the time series of y would show no pulses unless it was very long.

To quantify the qualitative picture just given we examine the statistical properties of the solution to (4.2). The probability, $p(y, t)dy$, that the salinity gradient assumes a value in the range $[y, y + dy]$ at time t, is determined by the Fokker–Planck equation (Gardiner 1985)

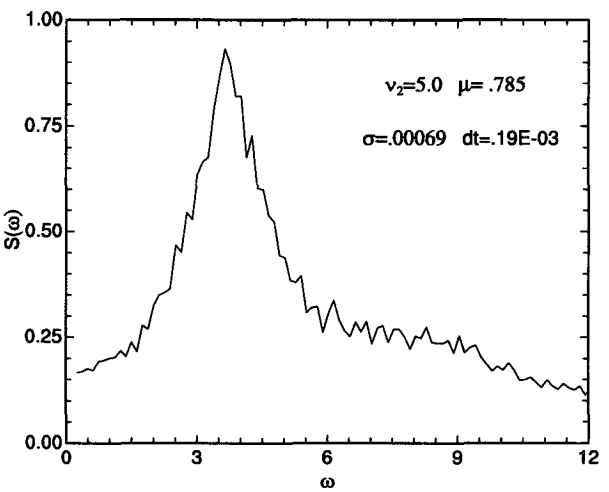

FIG. 7. The spectrum obtained by averaging 200 numerical solutions of (4.2) for different realizations of the stochastic fluctuations $\mu'(t)$. For each realization $\bar{\mu} = 0.785$, $\nu_2 = 5.0$, $y_{max} = 0.252$, $\mu_2 = 0.78\overline{3}$ and $\sigma = 0.000690535$. The criticality is $\delta = -0.000\overline{3}$, and the spread of the distribution is $\Delta = 0.0003088$. Even if δ is slightly greater than Δ, the prediction (4.13) for the center frequency of the peak ω_c is satisfactory (it gives $\omega_c \sim 3.89$).

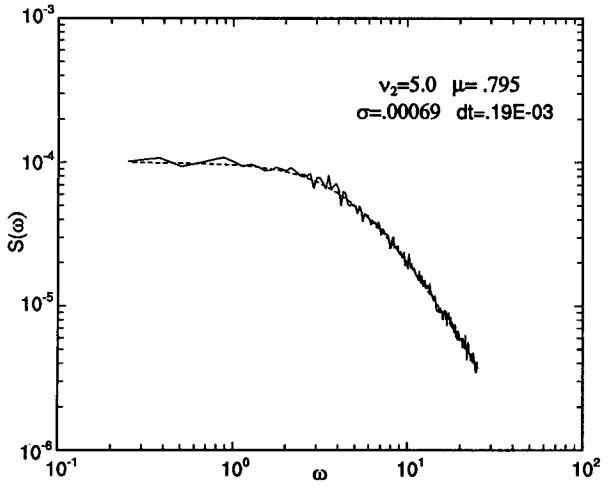

FIG. 8. The spectrum obtained by averaging 200 numerical solutions of (4.2) for different realizations of the stochastic fluctuations $\mu'(t)$ (solid line). For each realization $\bar{\mu} = 0.795$, and $\sigma = 0.000690535$. The other parameters are as in Fig. 7. The criticality is $\delta = -0.002\bar{3}$ and the spread of the distribution is $\Delta = 0.0003088$. The prediction (4.15) is plotted as a dashed line.

$$\partial_t p = \partial_y J(y, t), \tag{4.6}$$

with the probability flux, $J(y, t)$, given by

$$J(y, t) \equiv (\nu_2 y - \bar{\mu})p(y, t) + \sigma^2 \partial_y p(y, t)/2. \tag{4.7}$$

The prescription of instantaneous adjustment when the salinity gradient falls below the convecting threshold enters the Fokker–Planck equation through the boundary conditions

$$p(y \leqslant \mu_2/\nu_2, t) = 0,$$
$$J(\mu_2/\nu_2, t) = J(y_{\max}, t). \tag{4.8}$$

The boundary conditions state that no value of y below μ_2/ν_2 is allowed and that the ensemble members "lost" at μ_2/ν_2 through random diffusion are reinjected at $y_{\max}$.

To determine the probability density function (PDF) $p(y, t)$, the additional normalization condition is imposed:

$$\int_{\mu_2/\nu_2}^{y_{\max}} p(y, t)dy = 1. \tag{4.9}$$

For weak stochastic agitation, where pulses are an identifiable entity, the value of the probability flux at the boundary, $J(y_{\max}, t)$, is equal to the number of pulses per unit time in the time series shown in Fig. 6, and, in general, this frequency is found by solving the system (4.6)–(4.9) from arbitrary initial conditions. However, for a long enough time series, where the memory of the initial state is lost, the PDF reaches a time-independent distribution $p_s(y)$, which is a solution of the stationary Fokker–Planck equation. In the steady state J is a constant, independent of y as well as t. The stationary distribution is

$$p_s(y) = 2\sigma^{-2} J(y_{\max}) \exp\left[-\frac{\nu_2}{\sigma^2}\left(y - \frac{\bar{\mu}}{\nu_2}\right)^2\right] \times \int_{\mu_2/\nu_2}^{y} dy' \exp\left[\frac{\nu_2}{\sigma^2}\left(y' - \frac{\bar{\mu}}{\nu_2}\right)^2\right]. \tag{4.10}$$

The stationary probability flux J is determined by the normalization condition (4.9) and gives the *average* number of pulses per unit time

$$J(y_{\max}) = \nu_2\left[2\int_{\delta/\Delta}^{(y_{\max} - \mu_2/\nu_2 + \delta)/\Delta} \exp(-y^2)dy \times \int_{\delta/\Delta}^{y} \exp(y'^2)dy'\right]^{-1}; \tag{4.11}$$

δ is the distance to the critical value of the parameter, defined in section 2, and Δ is defined in (4.5).

Even when considering Δ and δ both to be much less than one, the average frequency of pulses, $J(y_{\max})$, depends on the relative ordering of the two small parameters. If $\delta \ll \Delta$, pulses are frequent and the salinity gradient is quasi periodic in time as in Fig. 6. The spectrum of y then shows a peak centered around the average frequency $2\pi J(y_{\max})$, as typified in Fig. 7. In this case $J(y_{\max})$ can be approximated with

$$J(y_{\max}) \approx \nu_2\left[2\int_0^{(y_{\max} - \bar{\mu}/\nu_2)/\Delta} D(y)dy + O(\delta/\Delta)\right]^{-1}, \quad (\delta \ll \Delta). \tag{4.12}$$

In (4.12) $D(y)$ is the Dawson's integral (Abramowitz and Stegun 1965, p. 297).

If we further assume that $y_{\max} - \bar{\mu}/\nu_2 \gg \Delta$, then we can replace the Dawson integral with its asymptotic expansion for large argument, $D(y) \approx (2y)^{-1}$. To leading order the probability flux is given by $J(y_{\max}) \approx -\nu_2/\ln\Delta$ and the center frequency, ω_c, of the spectrum depends to zeroth order on the noise amplitude; that is,

$$\omega_c = 2\pi J(y_{\max}) \approx -2\pi\nu_2/\ln\Delta. \tag{4.13}$$

Comparing the approximate value of the center frequency, (4.13), with the formula for the period τ, in (3.3), shows that the frequency of oscillation for the stochastically forced system, for *negative* criticality $\delta \ll \Delta$, has the same dependence on the noise amplitude Δ that the frequency of oscillation of the associated deterministic system, $2\pi/\tau$, has on the *positive* criticality δ. In other words, for this nonlinear system the noise acts to "shift" the mean salinity flux $\bar{\mu}$ past the threshold leading to oscillations by an amount proportional to the square root of the variance. Once again, this is not a peculiar property of the "adjustment" scheme (3.1), or of Welander's flip–flop, but is a ge-

neric feature of systems near the threshold of hard loss of stability and subject to noise (e.g., Gang et al. 1993).

If $\Delta \ll |\delta| \ll y_{\max} - \mu_2/\nu_2$, the system is almost always in the convective state and pulses of interrupted convection occur at an exponentially small rate. In this case, we can approximate the integral (4.11) with its asymptotic leading behavior as $\delta/\Delta \to -\infty$ and $(y_{\max} - \mu_2/\nu_2 + \delta)/\Delta \to \infty$. In this limit the average number of pulses per unit time, $J(y_{\max})$, is

$$J(y_{\max}) \approx -\nu_2 \exp(-\delta^2/\Delta^2)\delta/(\Delta\sqrt{\pi}). \quad (4.14)$$

When the pulses occur at such a small rate, they can be neglected, and the stochastically forced system (4.2) is the usual Orstein–Uhlenbeck process. Then the spectrum of the salinity gradient y has no peaks and is given by

$$S(\omega) \equiv \int_{-\infty}^{+\infty} \langle (y(t) - \langle y \rangle)(y(s+t) - \langle y \rangle) \rangle e^{-i\omega t} dt = \frac{\sigma^2}{dt(\omega^2 + \nu_2^2)}. \quad (4.15)$$

Figure 8 shows that the spectrum obtained from numerical integration of the adjustment model (4.2), for a choice of parameters satisfying $\Delta \ll |\delta| \ll 1$, is well approximated by (4.15). In this regime the spectrum has no peaks: the variance of the noise is too small to induce pulses frequently enough for quasi-periodic behavior. Notice that a 1.3% increase in the value of $\bar{\mu}$ (keeping the noise variance Δ fixed) produces a decrease by a factor of 10^{-4} in the amplitude of the spectrum (cf. the vertical axes of Figs. 7 and 8).

The dependence of the peak frequency of the spectrum on the noise amplitude (4.13) should be contrasted with that obtained in the stochastically forced weakly damped, weakly nonlinear oscillator, which to zeroth order is independent of the variance of the noise. In particular, when the noise is much smaller than the damping rate, the nonlinear effects can be neglected and the damped oscillator forced by white noise is

$$\ddot{y} - \delta\dot{y} + \Omega^2 y = \mu'(t) \quad (4.16)$$

(here $\delta < 0$ so that the damping is positive). The spectrum of the damped harmonic oscillator can be easily calculated taking the Fourier transform of (4.16) and is given by

$$S(\omega) = \frac{\sigma^2}{dt[(\omega^2 - \Omega^2)^2 + \delta^2\omega^2]}; \quad (4.17)$$

that is, the peak of the spectrum, at $\omega_c = (\Omega^2 - \delta^2/2)^{1/2}$, is still very close to the intrinsic frequency, Ω. Notice that a spectrum such as that in Fig. 7, could be accurately fitted to the form (4.17), appropriate for the excitation by noise of a damped system with a linear eigenfrequency. However, the time series of the two processes are distinctly different, as is the dependence of the spectrum on the noise amplitude. Thus in this case an accurate fit of the spectrum has no physical significance.

All of the preceding discussion is focussed on the case in which the deterministic system settles into a steady state. But it is easy to see what would happen if stochastic forcing was added to a deterministic system operating just inside the oscillatory regime. The stochastic fluctuation will kick the system past the adjustment threshold before the deterministic dynamics would reach it. Thus, the effect of the stochastic forcing is to decrease the period of the oscillations.

In summary, the fourth point of contact between (4.2) and the general circulation models mentioned in the introduction is that the frequency of the thermohaline oscillations increases when the variance of the stochastic component of the freshwater flux increases (cf. Fig. 13 of Weaver et al. 1993), while the amplitude of the oscillations does not.

5. Summary and conclusions

In this paper we contrasted two types of loss of stability, "hard" versus "soft," and emphasized that the Welander flip–flop model exhibits the hard type, characterized by a continuous variation of the period as the transition threshold is approached. Specifically the Welander flip–flop model exhibits a logarithmic dependence of the period on the freshwater flux. Also, even just past the transition threshold the oscillations have finite amplitude that is essentially independent of the freshwater flux.

The sensitivity of the period of the oscillations found in OGCMs to small changes in the freshwater flux (Weaver et al. 1993; Huang and Chow 1994; Pierce et al. 1995) and to the precise formulation of convective adjustment schemes (Marotzke 1991; Yin and Sarachik 1994), suggests that hard loss of stability is typical of thermohaline oscillations found in many OGCMs. This conjecture suggests quantitative verification of the prediction that the period depends logarithmically on the distance to criticality. Although discouraging for those hoping to predict the variability of climate, this sensitivity might accurately portray the delicacy of deep-water formation processes in high-latitude oceans.

The differences between a hard and a soft transition are mirrored when considering quasi-periodic behavior excited by stochastic forcing. In the hard case the center frequency of the spectrum depends on the variance of the noise, decreasing with the noise amplitude. The noise-induced oscillation is in the form of a sequence of pulses, each of constant, finite amplitude excursion. Moreover, the noise-induced quasi-periodic behavior is lost when the variance falls below a threshold value. This phenomenology is reproduced in OGCMs subject to stochastic fluctuations (Mikolajewicz and Maier-Reimer 1990; Weaver et al. 1993), indicating that the present class of OGCMs is operating in a very excitable region of parameter space.

Acknowledgments. Numerous conversations with Bill Young and Olivier Thual are gratefully acknowledged. Funding for this research is provided by the Department of Energy through its CHAMMP Program (DOE DEFG03 93ER61690) and by the Commission of the European Communities through its MAST II Programme (MAS2-CT-92-0034).

APPENDIX

Approximate Calculation of the Period of Oscillation of Welander's Flip–Flop Oscillator

In this appendix we calculate the approximate period of the periodic solutions of the system (2.5) and (2.7) assuming that the nondimensional salinity flux μ is just a little bit smaller than μ_2 defined in (2.8). In other words we consider the parameter

$$\delta \equiv (\mu_2 - \mu)/\nu_2 \tag{A.1}$$

to be positive and much smaller than unity. For negative δ the system (2.5) reaches the fixed point, $x = 1/(1 + \nu_2)$, $y = \mu/\nu_2$, where convection is always active.

When δ is positive and small, the oscillation, as shown in Fig. 1, consists of a relaxation towards the fixed point found for negative δ and a fast jump away from it. At the beginning and end of each phase the density gradient, $y - x$, is equal to ϵ. During the relaxation, convection is active, and the temperature and salinity gradients obey

$$\dot{x} = 1 - (1 + \nu_2)x$$
$$\dot{y} = \mu - \nu_2 \tag{A.2}$$

with initial condition

$$x(0) = y_{\max} - \epsilon, \quad y(0) = y_{\max}. \tag{A.3}$$

Because the jump (when convection is halted) at the end of the relaxation phase is very short when $\delta \ll 1$, the period τ of the relaxation–oscillation is approximately given by the time taken by the density gradient $y - x$ to reach the threshold value ϵ again during the relaxation. The density gradient solution of (A.2) with initial conditions (A.3) is

$$y - x = \mu/\nu_2 - 1/(1 + \nu_2) + e^{-\nu_2 t}[y_{\max} - \mu/\nu_2 + e^{-t}(\mu_2/\nu_2 - y_{\max})]. \tag{A.4}$$

The condition $y(\tau) - x(\tau) = \epsilon$ determines the approximate period, and it gives a transcendental equation, which can be approximately solved using the iteration scheme

$$e^{-\nu_2 \tau_n} = \delta[y_{\max} - \mu/\nu_2 + e^{-\tau_{n-1}}(\mu_2/\nu_2 - y_{\max})]^{-1} \tag{A.5}$$

with $\tau_0 = \infty$. Equation (A.5) gives an accurate answer in a few iterations because τ is large when δ is small. Here we just give the answer obtained iterating (A.5) twice:

$$\tau \approx \tau_2 = -\nu_2^{-1}[\ln\delta - \ln(y_{\max} - \mu/\nu_2) + \delta^{1/\nu_2}(y_{\max} - \mu_2/\nu_2)(y_{\max} - \mu/\nu_2)^{-1-1/\nu_2}]. \tag{A.6}$$

The dominant term on the right-hand side of (A.6) is proportional to $\ln\delta$ when $\delta \ll 1$, as long as $y_{\max}$ is approximately a constant in the same limit. This is indeed the case as it will be shown later.

Despite the horrible appearance of (A.6), the value of the salinity gradient at the end of the relaxation phase is moderately simple and is given by

$$y_{\min} \approx y(\tau_2) = \mu_2/\nu_2 + \delta^{1+1/\nu_2}(y_{\max} - \mu_2/\nu_2)^{1/\nu_2}. \tag{A.7}$$

As expected, the salinity gradient at the end of the relaxation (convection) phase is close to the value of the fixed point found were δ is slightly negative.

We can now, at least in principle, calculate the value of the salinity gradient at the end of the brief nonconvective phase. During the short jump the temperature and salinity gradient satisfy

$$\dot{x} = 1 - (1 + \nu_1)x$$
$$\dot{y} = \mu - \nu_1 y \tag{A.8}$$

with initial condition

$$x(0) = y_{\min} - \epsilon, \quad y(0) = y_{\min}. \tag{A.9}$$

The approximate expression for $y_{\min}$ is given in (A.7), and $y_{\max}$ is the value of y at the end of the nonconvective phase, that is, when the density gradient $y - x$ reaches ϵ during the brief halting of convection. The density gradient solution of (A.8) is

$$y - x = (\mu - \mu_1)/\nu_1 + \epsilon + e^{-\nu_1 t}[y_{\min} - \mu/\nu_1 + e^{-t}(\mu_1/\nu_1 - y_{\min})]. \tag{A.10}$$

It initially decreases for $t \ll 1$ and then increases again, reaching a minimum. Thus $y_{\max}$ is equal to $y(t^*)$ where t^* is the time at which $y - x$ equals ϵ after reaching a minimum value. Several methods were used to attempt to find an approximate analytic expression for t^* and $y_{\max}$, but none gave a satisfactory solution. Approximate solutions, obtained numerically using (A.7) are given in Table 1.

The essential point is that when $\mu = \mu_2$ and $\delta = 0$, $y_{\max}$ reaches a constant value, larger than $y_{\min}$, so the amplitude of the oscillation is finite even at the boundary of the transition. Moreover, the duration t^* of the nonconvective phase is short compared to the relaxation time τ, given approximately in (A.6), which becomes infinite at the transition threshold.

REFERENCES

Abramowitz, M., and I. A. Stegun, 1965: *Handbook of Mathematical Functions.* Dover, 1046+xiv pp.

Andronov, A. A., A. A. Vitt, and S. E. Chaikin, 1966: *Theory of Oscillators.* Pergamon Press, 815+xxxii pp.

Arnol'd, V. I., 1992: *Catastrophe Theory.* Springer Verlag, 150+xiii pp.

Gang, H., T. Ditizinger, C. Z. Ning, and H. Haken, 1993: Stochastic resonance without external periodic force. *Phys. Rev. Lett.,* **71,** 807–810.

Gardiner, C. W., 1985: *Handbook of Stochastic Methods for Physics, Chemistry, and the Natural Sciences.* Springer-Verlag, 442+xix pp.

Huang, R. X., and R. L. Chou, 1994: Parameter sensitivity study of the saline circulation. *Climate Dyn.,* **9,** 391–409.

Jones, H., and J. Marshall, 1993: Convection with rotation in a neutral ocean—A study of open-ocean deep convection. *J. Phys. Oceanogr.,* **23,** 1009–1039.

Marotzke, J., 1991: Influence of convective adjustment on the stability of the thermohaline circulation. *J. Phys. Oceanogr.,* **21,** 903–907.

Mikolajewicz, U., and E. Maier-Reimer, 1990: Internal secular variability in an ocean general circulation model. *Climate Dyn.,* **4,** 145–156.

Pierce, D. W., T. P. Barnett, and U. Mikolajewicz, 1995: Competing role of heat and fresh water flux in forcing thermohaline oscillations. *J. Phys. Oceanogr.,* **25,** 2046–2064.

Weaver, A. J., J. Marotzke, P. F. Cummins, and E. S. Sarachik, 1993: Stability and variability of the thermohaline circulation. *J. Phys. Oceanogr.,* **23,** 39–60.

Welander, P., 1982: A simple heat–salt oscillator. *Dyn. Atmos. Oceans,* **6,** 233–242.

——, 1986: Thermohaline effects in the ocean circulation and related simple models. *Large-Scale Transport Processes in Oceans and Atmosphere,* NATO ASI Series, J. Willebrand and D. L. T. Anderson, Eds., Reidel, 163–200.

Winton, M., 1993: Deep decoupling oscillations of the oceanic thermohaline circulation. *Ice in the Climate System,* NATO ASI Series, Vol. 112, W. R. Peltier, Ed., Springer Verlag, 417–432.

Yang, J., and J. D. Neelin, 1993: Sea–ice interaction with the thermohaline circulation. *Geophys. Res. Lett.,* **20,** 217–220.

Yin, F. L., and E. S. Sarachick, 1994: An efficient convective adjustment scheme for ocean general circulation models. *J. Phys. Oceanogr.,* **24,** 1425–1430.